Chlorodifluoroacetyl Isocyanate, ClF2CC(O)NCO: Preparation, Structural and Spectroscopic Studies.

ARTICLE *in* THE JOURNAL OF PHYSICAL CHEMISTRY A · NOVEMBER 2012

Impact Factor: 2.69 · DOI: 10.1021/jp3096055 · Source: PubMed

THE JOURNAL OF PHYSICAL CHEMISTRY A

Article

pubs.acs.org/JPCA

Chlorodifluoroacetyl Isocyanate, $ClF_2CC(O)NCO$: Preparation and Structural and Spectroscopic Studies

Luis A. Ramos,[†] Sonia E. Ulic,[†] Rosana M. Romano,[†] Yury V. Vishnevskiy,[‡] Raphael J. F. Berger,[‡,#] Norbert W. Mitzel,[‡] Helmut Beckers,[§] Helge Willner,[§] Shengrui Tong,[∥] Maofa Ge,[∥] and Carlos O. Della Védova*[,†]

[†]CEQUINOR (UNLP-CONICET), Departamento de Química, Facultad de Ciencias Exactas, Universidad Nacional de La Plata, 47 esq. 115, 1900 La Plata, República Argentina

[‡]Lehrstuhl für Anorganische Chemie und Strukturchemie, Universität Bielefeld, Universitätsstraße 25, 33615 Bielefeld, Germany

[§]Fachbereich C - Anorganische Chemie, Bergische Universität Wuppertal, 42097 Wuppertal, Germany

[∥]State Key Laboratory for Structural Chemistry of Unstable and Stable Species, Institute of Chemistry, Chinese Academy of Sciences, Beijing 100190, China

Supporting Information

ABSTRACT: Chlorodifluoroacetyl isocyanate, $ClF_2CC(O)NCO$, was prepared by the reaction of $ClF_2CC(O)Cl$ with excess of AgNCO. The colorless compound melts at −83 °C and the vapor pressure follows the equation ln p = −3868.3 $(1/T)$ + 10.89 (p [Atm], T [K]) in the range −38 to +22 °C, extrapolated bp ca. 82 °C. It has been characterized by IR (gas phase, Ar matrix), liquid Raman, ^{19}F and ^{13}C NMR, gas UV−vis spectrum, photoelectron spectroscopy (PES), photoionization mass spectrometry (PIMS), and gas electron diffraction (GED). The matrix photochemistry has been studied and the conformational properties of $ClF_2CC(O)NCO$ have been analyzed by joint application of vibrational spectroscopy, GED, and quantum chemical calculations. Two conformers were detected in gaseous and liquid phases, in which the C−Cl bond adopts a gauche orientation with respect to the C═O group, whereas this group can be in syn or anti orientation with respect to the N═C bond of the NCO group. An enthalpy difference ΔH°_{exp} = 1.3 ± 0.2 kcal mol^{-1} between the most stable syn−gauche and the less stable anti-gauche form was derived using the van't Hoff equation, which is in reasonable agreement with the computed difference of ΔH° = 0.8 kcal mol^{-1} (B3LYP/6-311+G(3df) approximation). The most significant gas phase structural parameters for gauche−syn $ClF_2CC(O)NCO$ are r_e(NC═O) = 1.157(1) Å, r_e(N═CO) = 1.218(1) Å, r_e(N−C) = 1.378(9) Å, r_e(C═O) = 1.195(1) Å, $\angle_e$(CNC) = 128.6(19)°. Photolysis of $ClF_2CC(O)NCO$ using an ArF excimer laser (193 nm) mainly yield ClF_2CNCO along with some $ClF_2CC(O)N$ nitrene. The valence electronic properties of the title compound were studied using the PES and PIMS. The experimental first vertical ionization energy of 11.54 eV corresponds to the ejection of a carbonylic oxygen lone pair electron.

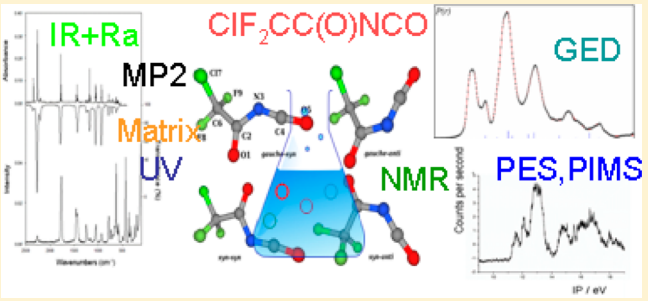

INTRODUCTION

Isocyanates, i.e., derivatives of the isocyanic acid, have a wide range of applications, but also present very basic challenges. They are precursors in the formation of polyurethane polymers and thus have a variety of important technological applications[1,2] including adhesives, sealants and paints, and flexible and rigid foams. However, fundamental aspects of the isocyanates are also of interest. Off-axis substitution on a pseudohalogen of the type azide, isothiocyanate, or isocyanate leads to interesting spectroscopic consequences caused by splitting of the π degeneration.[3]

Our fundamental studies on the bonding and properties of isocyanates containing molecules has included a large series of molecules: $S(NCO)_2$, $FC(O)NCO$, $ClC(O)NCO$, $BrC(O)NCO$, $CH_3C(O)NCO$, FSO_2NCO, $ClSO_2NCO$, CF_3SO_2NCO, $F_2NC(O)NCO$, $ClCH_2CH_2NCO$, $FC(O)SNCO$, $CH_3OC(O)SNCO$, $OV(NCO)_3$, $ONNCO$, N_3NCO, $FNCO$, and $CClF_2NCO$ (see refs 4−6 and references cited therein). These contributions include preparation, chemical, physical, and spectroscopic studies of the compounds. The molecule $ClC(O)NCO$ challenges the reliability of ab initio calculations.[7] The conformational properties of the molecules $XC(O)NCO$ (X = F, Cl, Br, and CH_3) are of interest: the *syn* conformation in equilibrium with a lower concentration of the anti form seems to be preferred for Cl, Br, and CH_3 compounds, whereas for $FC(O)NCO$ the anti rotamer (65%) is the most stable form. Very few molecules provide vibrational spectra so rich in information as $FC(O)NCO$.[8]

Received: September 27, 2012
Revised: November 1, 2012
Published: November 1, 2012

dx.doi.org/10.1021/jp3096055 | J. Phys. Chem. A 2012, 116, 11586−11595

Another interesting result concerning isocyanates is the mechanism of its UV photoevolution from carbonyl azides. Carbonyl azides can photoevolve to two different products, carbonyl nitrenes and the Curtius-rearranged isocyanate molecule.[9] Our interest covers also the electronic characteristics of the isocyanates, see for instance the PES study of $S(NCO)_2$ and the results derived by using this spectroscopy.[10] In the present work we will combine all these studies to gain a detailed understanding of the title species. Consequently, for chlorodifluoroacetyl isocyanate, $ClF_2CC(O)NCO$, we will report the results from an interdisciplinary study including its preparation, determination of physical properties, its IR (gas phase, Ar matrix), liquid Raman, ^{19}F and ^{13}C NMR, gas UV−vis spectrum, photoelectron spectroscopy (PES), photoionization mass spectrometry (PIMS), and gas electron diffraction (GED). These data will be reciprocally linked and complemented with results from computations to analyze its conformational and photochemical behavior along the photoelectron spectroscopy (PES) to determine molecular energy levels of $ClF_2CC(O)NCO$ in its valence region.

EXPERIMENTAL SECTION

Synthesis. Silver cyanate was prepared from $AgNO_3$ and KNCO, and $ClF_2CC(O)Cl$ was prepared by chlorination of the corresponding acid, $ClCF_2C(O)OH$, with PCl_5. $ClF_2CC(O)NCO$ was synthesized by the reaction of difluorochloroacetyl chloride, $ClF_2CC(O)Cl$, with excess of silver cyanate, AgNCO. For this purpose 1.2 g of $ClF_2CC(O)Cl$ were distilled into an evacuated 250 mL glass vessel provided with a Young valve and 1.5 g of dry AgNCO. The reaction was carried out for 2 h at 20 °C. The product was purified by trap-to-trap condensations with traps held at −60, −100, and −196 °C. $ClF_2CC(O)NCO$ remained in the trap at −60 °C together with a small amount of difluorochloroacetyl chloride, which was further separated by fractional distillation. The final yield was 60%.

Instrumentation and Procedure. *(a). General Procedure.* Volatile materials were manipulated in a glass vacuum line equipped with a capacitance pressure gauge (221 AHS-1000, MKS Baratron, Burlington, MA), three U-traps and valves with PTFE stems (Young, London, U.K.). The vacuum line was connected to an IR cell (optical path length 200 mm, Si windows 0.5 mm thick) placed in the sample compartment of a Bruker Vector 25 FTIR spectrometer. This arrangement allows to follow the course of the reactions and the purification processes. The pure compound was stored in flame-sealed glass ampules under liquid nitrogen in a long-term Dewar vessel. The ampules were opened with an ampule key at the vacuum line, an appropriate amount was taken out for the experiments, and then they were flame-sealed again.[11] The vapor pressures of samples were measured in a small vacuum line equipped with a calibrated capacitance pressure gauge (MKS Baratron, AHS-100) and a small sample reservoir in the temperature range between −38 and +22 °C.

The melting point of $ClF_2CC(O)NCO$ was determined in a flame-sealed 6 mm glass tube placed in a transparent Dewar vessel with cold ethanol. The temperature was increased at a rate of about 1 °C min^{-1} starting at −100 °C. The solid melts at −83 °C to a colorless liquid.

(b). Vibrational Spectroscopy. Infrared gas spectra were recorded on a Bruker Vector 25 spectrometer, with a resolution of 2 cm^{-1} in the range from 4000 to 400 cm^{-1}, using a glass cell with Si windows and optical path length of 200 mm.

Raman spectra of the neat liquid at room temperature were measured in flame-sealed capillaries (3 mm o.d.) on a Bruker RFS 106/S spectrometer, equipped with a 1064 nm Nd:YAG laser, in the region from 4000 to 100 cm^{-1} using 2 cm^{-1} of resolution.

(c). Matrix Isolation Experiments. For matrix isolation experiments $ClF_2CC(O)NCO$ was diluted with argon in a ratio of 1:2000 in a 1 L stainless-steel storage container. Small amounts (∼0.2 mmol) of this mixture were deposited within 10 min onto the cold matrix support (16 K, Rh-plated Cu-block) in a high vacuum. Temperature-dependent experiments were carried out by passing the gaseous sample-Ar mixtures through a quartz nozzle (1 mm i.d.), heated over a length of ∼10 mm with a platinum wire (0.25 mm o.d.) prior to deposition on the matrix support. The nozzle was held at 298 and 583 K. Photolysis experiments were carried out with an ArF excimer laser (Lambda-Physics 193 nm) and with a high-pressure mercury lamp (TQ150, Heraeus) by conducting the light through water-cooled quartz lenses combined with different cut off filters (Schott).

IR spectra of matrix isolated samples were recorded in a reflectance mode on a Bruker IFS 66v/S spectrometer using a transfer optic. An MCT detector and a KBr/Ge beam splitter were used in the wavenumber range 5000 to 530 cm^{-1}. For the spectra with apodized resolutions of 0.25 cm^{-1} and 200 scans were added. More details of the matrix apparatus are given elsewhere.[12]

(d). UV Spectroscopy. A UV−visible spectrum of gaseous $ClF_2CC(O)NCO$ was recorded using a glass cell equipped with quartz windows (10 cm optical path length) and a Lambda EZ210 UV/vis spectrometer (Perkin-Elmer). Measurements were carried out in the spectral region from 190 to 700 nm with a sampling interval of 1.0 nm, a scan speed of 200 nm min^{-1}, and a slit with of 2 nm.

(e). NMR Spectroscopy. For ^{13}C and ^{19}F NMR spectra, pure samples were flame-sealed in thin-walled 4 mm o.d. tubes and placed into 5 mm NMR tubes. The NMR spectra were recorded on a Bruker Avance 400 spectrometer at 100.6 and 376.5 MHz, respectively. The samples were held at 25 °C and C_6D_6 was used as an external lock and reference.

(f). Quantumchemical Calculations. DFT calculations were performed using the program package GAUSSIAN 03.[13] MP2[14] calculations have been carried out using the Firefly program.[15] The potential surface of internal rotations along the C2−C6 and C2−N3 in $ClF_2CC(O)NCO$ bonds has been calculated at the B3LYP/cc-pVTZ level of approximation[16−19] by optimizing the molecular geometry with fixed torsion angles N3−C2−C6−Cl7 and O1−C2−N3−C4 in range from 0 to 360 and step size of 10° (see Figure 2). In this way four stable conformations were found: gauche−syn, gauche−anti, syn−syn, and syn−anti (see Figure 1). Using the B3LYP/6-31G(d) and MP2(full)/aug-cc-pVTZ approximations full optimizations of all conformers were performed. Subsequent calculations of vibrational frequencies proved that all these forms are true minima. The obtained energies and geometrical parameters for gauche−syn and gauche−anti conformers are given in Tables 1 and 3, respectively.

To assign the PES of $ClF_2CC(O)NCO$, we applied the OVGF approach using the 6-311+G(d) basis set, which includes correlation effects of the self-energy to the molecules to give accurate results of the vertical ionization energies.[20] Molecular orbital plots were generated using the Gauss View program.

dx.doi.org/10.1021/jp3096055 | J. Phys. Chem. A 2012, 116, 11586−11595

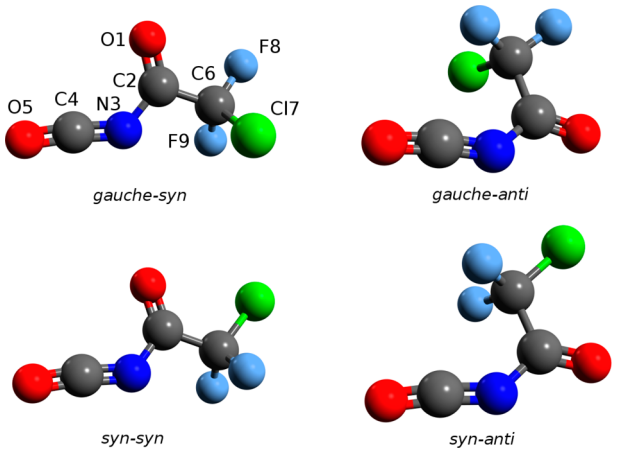

Figure 1. Conformations of $ClF_2CC(O)NCO$ calculated with the B3LYP/6-31G(d) level of approximation.

(g). Photoelectron and Photoionization Mass Spectroscopy. The equipment used in this work has been described previously.[21,22] The photoelectron and photoionization mass-spectrometer consists of two parts: the double-chamber UPS-II machine and a time-of-flight mass spectrometer. The PES was recorded in the double chamber UPS-II equipment with a resolution of about 30 meV as indicated by the Ar^+ ($^2P_{3/2}$) photoelectron band. Experimental vertical ionization energies (IPs) were calibrated by the simultaneous addition of a small amount of argon and methyl iodide to the sample. Mass analysis of ions was performed with the time-of-flight mass analyzer mounted directly to the photoionization point. The relatively soft ionization is provided by single-wavelength He(I) radiation. The PE and PIM spectra can be recorded subsequently within a few seconds under identical conditions.

(h). Gas Electron Diffraction. The electron diffraction patterns were recorded on the heavily improved Balzers Eldigraph KD-G2 gas-phase electron diffractometer[23] at the University of Bielefeld. The experimental details are presented in Table 7. In total two images for each, the long and short nozzle-to-plate distances, were measured on the Fuji BAS-IP MP 2025 imaging plates. The plates with the diffraction patterns were scanned using a calibrated Fuji BAS-1800II scanner. The intensity curves (Figure S5) were obtained by applying the method described earlier.[24] Sector function and electron wavelengths were estimated using the method described in the literature,[25] from benzene diffraction patterns, recorded along with the substance under investigation.

In order to compute amplitudes of vibrations and curvilinear corrections used in the gas-phase electron diffraction refinements, analytical quadratic and numerical cubic force fields were calculated for both gauche−syn and gauche−anti conformers employing the B3LYP/6-31G(d) approximation. The mean square amplitudes and vibrational corrections to the equilibrium structure were calculated with the SHRINK program.[26−29] Root mean square amplitudes were refined in groups (see Tables S1 and S2). For this purpose the scale factors (one per group) were used as independent parameters. Thus, the ratios between different amplitudes in one group were fixed at the theoretical values calculated from B3LYP/6-31G(d) quadratic and cubic force fields.

RESULTS AND DISCUSSION

General Properties. Solid $ClF_2CC(O)NCO$ melts at −83 °C to a colorless liquid. The vapor pressure of the liquid was measured over a temperature range between −38 and +22 °C. Its temperature dependence can be described by the eq 1 from which a boiling point of 82 °C was extrapolated. $ClF_2CC(O)NCO$ is stable at room temperature.

$$\ln p = -3868.3(1/T) + 10.89(p[\mathrm{Atm}],\ T[\mathrm{K}]) \quad (1)$$

The ambient temperature ^{19}F NMR spectrum shows a singlet at δ = −65.8 ppm attributed to both fluorine atoms of the $ClCF_2$ group (Figure S1, Supporting Information). The ^{13}C NMR spectrum exhibits two triplet signals at δ = 157.6 ppm ($^2J_{C-F}$ = 37.3 Hz) and δ = 117.9 ppm ($^1J_{C-F}$ = 301.5 Hz) and a singlet at 131.4 ppm, corresponding to the carbon atoms of the C═O, $ClCF_2$ and NCO groups, respectively (Figure S2, Supporting Information). These values are in good agreement with those reported for similar compounds.[30] The UV−visible spectrum of gaseous $ClF_2CC(O)NCO$ (Figure S3, Supporting Information) shows an absorption band at λ_{max} = 256 nm attributed to the n → π^* transition located on the C═O carbonyl chromophore and a stronger absorption at λ_{max} = 197 nm, which could be due to the π → π^* transition on this chromophore, according to reports for similar molecules.[30] Figures showing the UV−visible spectra of $CClF_2C(O)NCS$[31] and $CClF_2C(O)N_3$[6] are included for comparison.

Computational chemistry. The presence of both, a chlorine atom and an NCO group, in $ClF_2CC(O)NCO$ raises the possibility to adopt more than one orientation around the C2−C6 and C2−N3 bonds (Figure 1). To evaluate the expected conformational equilibrium, a potential energy surface for the internal rotation about both bonds was calculated at the B3LYP/cc-pVTZ level of theory (Figure 2). In addition a full optimization of all possible conformers on the potential energy surface of $ClF_2CC(O)NCO$ was carried out using ab initio (MP2) and DFT (B3LYP) levels of theory. Four conformers, denoted as gauche−syn, gauche−anti, syn−syn, and syn−anti (Figure 1), were found to correspond to minima over the potential energy surface (Figure 2). The calculated energies of

Table 1. Calculated Relative Energies and Estimated Abundances of the $ClF_2CC(O)NCO$ Conformers at 298, 478, and 583 K[a]

	B3LYP/6-31G(d)				MP2(full)/aug-cc-pVTZ			
	g-s	g-a	s-s	s-a	g-s	g-a	s-s	s-a
ΔE, kcal/mol	0.00	0.87	1.42	1.81	0.00	0.13	1.23	1.21
$\Delta G°$, kcal/mol	0.00	0.84	1.11	1.46	0.00	0.27	1.03	1.18
x^b, % (298 K)	73	18	6	3	56	35	5	4
x^b, % (478 K)	60	25	9	6	48	37	8	7
x^b, % (583 K)	55	26	11	8	46	36	10	8

[a]g-s, g-a, s-s, and s-a denote the gauche−syn, gauche−anti, syn−syn, and syn−anti conformations, respectively. [b]Calculated from $\Delta G°$ according to the Boltzmann law at 298, 478, and 583 K.

dx.doi.org/10.1021/jp3096055 | J. Phys. Chem. A 2012, 116, 11586−11595

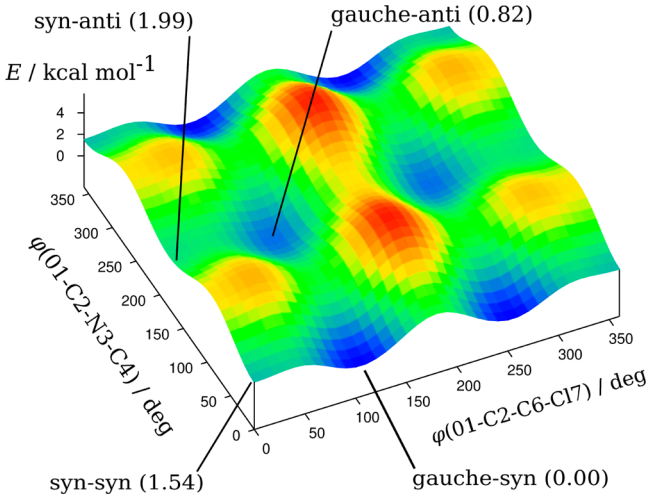

Figure 2. Potential surface for rotation along bonds C2−C6 and C2−C3 calculated at the B3LYP/cc-pVTZ level of theory.

these rotamers and their estimated abundances at room temperature are given in Table 1. The gauche−syn conformer was predicted to be more stable than the gauche−anti form at both levels of theory. The energy differences of the more stable forms gauche−syn and gauche−anti, however, vary from 0.84 kcal mol^{-1} (B3LYP/6-31G(d)) to 0.27 kcal mol^{-1} (MP2(full)/aug-cc-pVTZ) (4.18 J = 1 cal). Thus, a contribution of more than 15% of the gauche−anti conformer in the gas phase at 298 K can be estimated according the calculated Gibbs free energy difference between the two forms. Additionally, the abundances of both syn−syn and syn−anti conformers are less than 10% according to the calculations.

Vibrational Spectra. Gas-phase IR, argon matrix IR, and liquid Raman spectra of $ClF_2CC(O)NCO$ are shown in Figure 3. The observed vibrational frequencies are listed in Table 2 and compared with the calculated frequencies of the two possible conformers at the B3LYP/6-311+G(3df) level of theory. $ClF_2CC(O)NCO$ has 21 fundamental vibrational modes which are expected to be active in IR and Raman.

For this compound the most interesting vibrational information appears in the carbonylic region. The position of the C═O stretching vibration can serve as conformational sensor for the molecule. This mode can be assigned straightforward to the strong signals at 1783 and 1761 cm^{-1} in the gas IR and liquid Raman spectra, respectively. A shoulder at 1775 cm^{-1} in the Raman spectrum becomes also apparent. As mentioned earlier in the computational section, two rotamers with gauche−syn and gauche−anti orientations are expected for the molecule. In such a case, the matrix-isolation technique is particularly well suited for studying the conformational equilibrium, due to the sharpness of the IR absorption bands of species isolated in inert solid matrixes. $ClF_2CC(O)NCO$ was isolated in argon (1:2000) and deposited onto the cold matrix support at 15 K. The recorded matrix IR spectrum is shown in Figure 3 (upper trace). Relevant conformational splitting were detected, in agreement with the results expected from the Raman spectra and computational chemistry. In order to confirm the presence of a conformational equilibrium, the temperature dependence of the matrix IR absorptions for equilibrium mixtures at 298 and 583 K were recorded in the NCO antisymmetric, CO, NCO symmetric and $CClF_2$ symmetric and antisymmetric normal modes of vibration

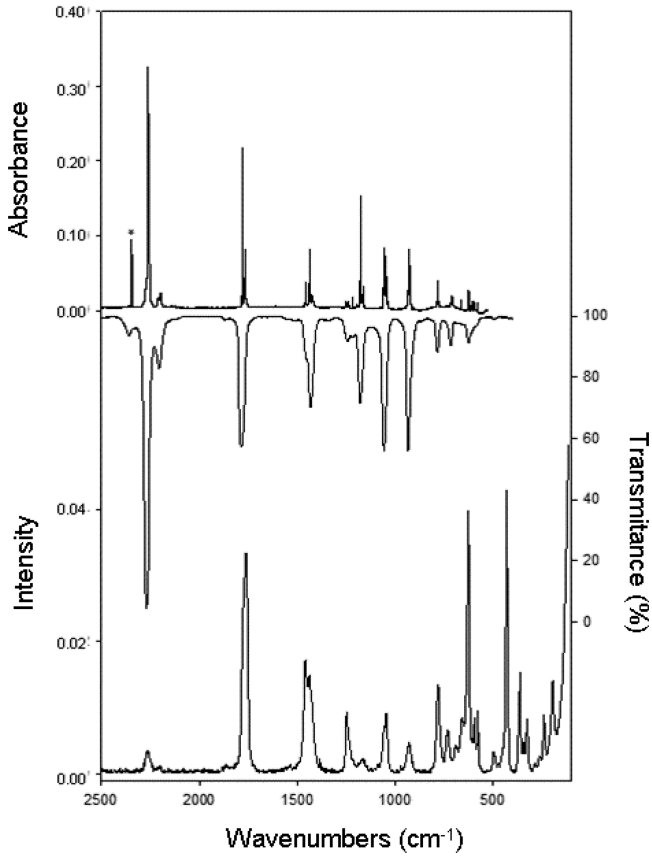

Figure 3. Upper trace: IR spectrum of $ClF_2CC(O)NCO$ isolated in an argon matrix (1:2000) at 16 K (resolution: 0.25 cm^{-1}). Middle trace: IR spectrum of gaseous $ClF_2CC(O)NCO$ at 298 K (resolution: 2 cm^{-1}). Lower trace: Raman spectrum of liquid $ClF_2CC(O)NCO$ at 298 K (resolution: 2 cm^{-1}). Band due to impurity is marked by an asterisk.

regions (see Figure 4 and Table 1 for the estimated populations at 478 and 583 K).

Accordingly, these matrix IR spectra revealed that the relative intensity of the bands attributed to the gauche−anti conformation increases with temperature, whereas the relative intensity of the corresponding bands of the gauche−syn form decreases. This indicates that gauche−syn is the most stable conformer, but also tells that it is in equilibrium with another less populated gauche−anti rotamer.

The remaining vibrational bands were assigned by comparison with reported data for related molecules.[6,8,30]

Using the results from Figure 4 and including the spectrum at 478 K an experimental ΔH°_{exp} = 1.3 ± 0.2 kcal mol^{-1} was derived using the van't Hoff equation for the enthalpy difference of these two rotamers with an estimated ΔS° = 0.10 cal K^{-1} mol^{-1} (B3LYP/6-311+G(3df)).

Photolysis of $ClF_2CC(O)NCO$. The UV spectrum of gaseous $ClF_2CC(O)NCO$ is depicted in Figure S3 (Supporting Information); it shows intense and weak absorptions at 197 and 256 nm, respectively, that are suitable to initiate UV photolysis processes.

When the matrix containing $ClF_2CC(O)NCO$ is irradiated for 6 min with light of a wavelength longer than 225 nm no sign of photoevolution was detected. However, 20 min of UV irradiation with λ = 193 nm (ArF laser, 2 mJ) induced the complete depletion of the IR bands of $ClF_2CC(O)NCO$. The IR difference spectrum showing the spectral changes during

dx.doi.org/10.1021/jp3096055 | J. Phys. Chem. A 2012, 116, 11586−11595

Table 2. Experimental and calculated frequencies (cm^{-1}) and assignments of the fundamental vibrational modes of $ClF_2CC(O)NCO$

	experimental				calculated[d]		
mode	IR (gas)[a]	IR (Ar matrix)[b]	Raman (liquid)[c]		gauche−syn	gauche−anti	assignment[e]
ν_1	2269 vs	2260.2	2260	(8)	2335 (1333)	2346 (1178)	ν_{as}(NCO)
		2256.1					
ν_2	1783 s	1779.6	1775 sh	(76)	1815 (297)	1834 (547)	ν(C═O)
		1766.7	1761				
ν_3	1457 sh	1457.6	1458	(39)	1483 (260)	1502 (116)	ν_s(NCO), ν(C−N)
	1431 m	1436.7	1440 sh	(34)			
ν_4	1244 w	1252.6	1247	(21)	1243 (39)	1228 (69)	ν(C−C), $\nu_{as}(CF_2)$
		1241.3					
ν_5	1179 m	1177.6	1168	(6)	1164 (198)	1150 (158)	$\nu_{as}(CF_2)$
		1163.7					
ν_6	1057 s	1057.6	1055 sh	(17)	1048 (323)	1047 (235)	$\nu_s(CF_2)$, ν(C−N)
		1046.5	1045	(21)			
ν_7	933 s	930.9	931	(10)	919 (186)	911 (201)	$\nu_{as}(CF_2)$, ν(C−N)
		925.8	924 sh	(11)			
ν_8	785 w	782.8	781	(31)	788 (70)	738 (19)	ν(C−N), $\nu_s(CF_2)$, δ(NCO)
			737 sh	(14)			
ν_9	717 w	710.0	730	(15)	718 (86)	665 (18)	δ(CC(O)N)
ν_{10}					632 (41)	625 (22)	δ(NCO)
ν_{11}	624 w	624.8	627	(93)	617 (10)	613 (52)	$\delta(CF_2)$, δ(NCO)
ν_{12}		599.0	596	(21)	589 (9)	599 (13)	δ(NCO)
		578.0	579	(23)			
ν_{13}	491 vw		494	(8)	493 (6)	502 (3)	$\delta(CF_2)$
ν_{14}			431	(100)	421 (<1)	421 (<1)	ν(C−Cl), $\delta(CF_2)$
ν_{15}			369 sh	(36)	358 (2)	366 (2)	δ(CC(O)N)
			363				
ν_{16}			344	(13)	321 (<1)	338 (3)	$\rho(CClF_2)$
			327	(19)			
ν_{17}			264	(8)	239 (1)	263 (6)	$\rho(CClF_2)$
			241	(21)			
ν_{18}			197	(34)	188 (1)	188 (1)	δ(CCN), δ(ClCC)
ν_{19}					98 (<1)	96 (1)	δ(CNC)
ν_{20}					75 (1)	93 (<1)	τ((O)C−NCO)
ν_{21}					40 (<1)	25 (<1)	$\tau(CClF_2$−C(O))

[a]Relative band intensities: s, strong; m, medium strong; w, weak; v, very; sh, shoulder. [b]Only the most populated Ar-matrix sites are given. [c]Relative intensities based on the integrated band areas are given in the parentheses. sh, shoulder. [d]B3LYP/6-311+G(3df) calculated IR frequencies (cm^{-1}) and intensities in parentheses (km mol^{-1}). [e]ν, δ, ρ, and τ denote stretching, deformation, rocking, and torsion modes, respectively.

ArF laser photolysis is displayed in Figure 5 (lower trace). In Figure 5 (upper trace) the photodecomposition of $ClF_2CC(O)N_3$ is shown for comparison.[6] Apparently, the main photochannels are almost the same. In the present study both the formation of the nitrene, $ClF_2CC(O)N$, and isocyanate, ClF_2CNCO, along with CO were obtained by ArF laser photolysis of $ClF_2CC(O)NCO$. Assignments are collected in Table 3.

Gas Electron Diffraction Analysis. Gas electron diffraction was used to determine the gas-phase structure of $ClF_2CC(O)NCO$. The structural analysis was performed employing the UNEX program.[33] All refinements were performed using two intensity curves simultaneously (provided in Figure S4, Supporting Information), one from short and another from long camera distance, which were obtained by averaging independent intensity curves obtained in the experiment. For the definition of the independent geometrical parameters and their groups in least-squares refinements see Table 4. The differences between values of parameters in one group were kept fixed on the values taken from MP2(full)/aug-cc-pVTZ calculations.

In order to describe the conformational behavior of $ClF_2CC(O)NCO$ by means of the GED data the following models were evaluated. The one-conformer model for the gauche−syn, gauche−anti, syn−syn, and syn−anti gave total structural R_{str} factors of 5.8, 7.4, 9.7, and 11.5% respectively. The refinement of the two-conformer model consisting of the mixture of the gauche−syn and gauche−anti conformations gave R_{str} factor of 5.4% and 72(7)% of the gauche−syn form. The next was the four-conformer model. The refinement of ratios of all conformations leads to unstable solutions with very high correlations between parameters. A stable solution was obtained after fixing the relative abundance of both syn−syn and syn−anti forms to 5%, whereas the ratio of the gauche−syn and gauche−anti conformations were kept free to refine. This model gave larger R_{str} (5.8%) and a slightly worse agreement regarding the radial distribution function (see Figure 6). Thus, on the basis of electron diffraction data it is impossible to prove the existence of syn−syn and syn−anti conformations in the gas phase at the temperature of the experiment since their inclusion in the model did not lead to any significant improvement of the fit. Therefore, the two-conformer model with R_{str} = 5.4% was

dx.doi.org/10.1021/jp3096055 | J. Phys. Chem. A 2012, 116, 11586−11595

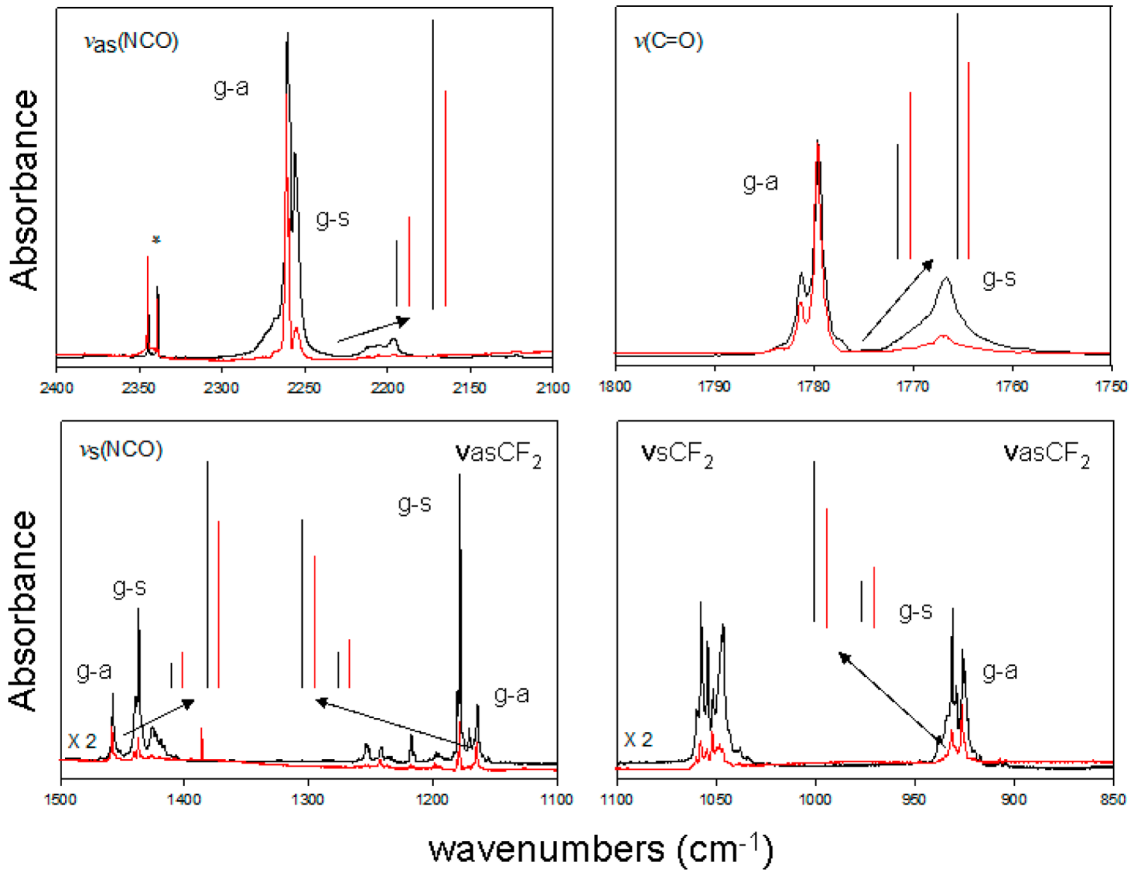

Figure 4. Ar matrix IR spectra (1:2000) in the regions of the ν_{as}(NCO), ν(CO), ν_{s}(NCO), ν_{s}(CF_2), and ν_{as}(CF_2) stretching fundamentals of an equilibrium mixture of gauche−syn and gauche−anti $ClF_2CC(O)NCO$ held at 298 K (black line) and at 583 K (red line) rapidly trapped in solid argon at 16 K. Stick-style calculated spectra for the two conformers using the B3LYP/6-311+G(3df) level of approximation intensities weighted by the conformer's estimated populations at the two temperatures according Table 1 are also depicted.

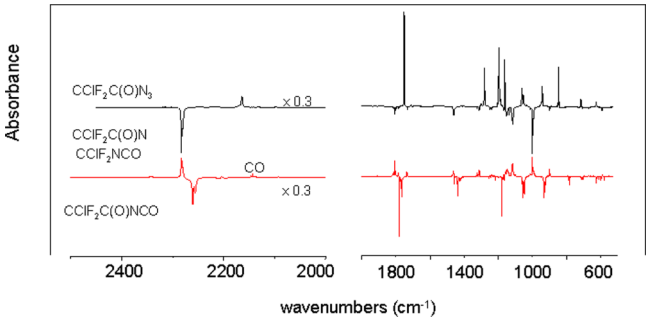

Figure 5. Lower trace: IR difference spectrum recorded before and after 20 min of an excimer laser irradiation (λ = 193 nm) of Ar-matrix isolated $ClF_2CC(O)NCO$. The IR bands of newly formed species point upward while those of depleted $ClF_2CC(O)NCO$ point downward. Uper trace: IR difference spectrum recorded before and after 10 min of UV−visible irradiation (λ > 225 nm) of Ar-matrix isolated $ClF_2CC(O)N_3$.

finally chosen. Its refinement gives the results shown in Table 4. The largest correlations were (i) −0.74 between parameters in groups 10 and 11 and (ii) −0.72 between parameters in groups 2 and 5 (see Table 4).

The structural parameters obtained for $ClF_2CC(O)NCO$ can be compared to a number of related compounds, HNCO,[34] $H_3CC(O)NCO$,[35] FC(O)NCO,[36] and ClC(O)NCO,[7] and a detailed listing of selected parameters is provided in Table 5. The length of the isocyanate C═O bond in $ClF_2CC(O)NCO$ is similar to those of $H_3CC(O)NCO$ and FC(O)NCO, but longer than that of ClC(O)NCO and shorter than that of HNCO. This is surprising, as the isocyanate N═C bond is of similar length for all the compounds and much closer to the different substituents. All C−N bonds between carbonyl group and NCO unit are much shorter than a typical single N−C bond (1.46 Å), the longest of this series is found for $H_3CC(O)NCO$, whereas electronegative F, Cl, or Cl_2FC substituents shorten this bonds.

Some variation is observed for the parameters describing the angle of the almost linear NCO group at the central N-atom, the angle C−N−C (or H−N−C in the case of HNCO). The smallest value of 123.11(15)° is found for HNCO. All carbonyl isocyanates have values of ≥125.9°, the maximum being 128.6(19)° for $ClF_2CC(O)NCO$.

Photoelectron Spectra. Photoelectron spectroscopy (PES) using He(I) radiation (21.2 eV = 58.4 nm) is an useful technique to study the valence electronic structure of molecules in combination with theoretical calculations.[37−39] The He(I) photoelectron spectrum of $ClF_2CC(O)NCO$ is shown in Figure 7. Outer valence Green function (OVGF) calculations were performed to obtain the ionization energies in order to assign the PE spectrum. The experimental vertical ionization potentials (IP), theoretical vertical ionization energies (E_v; OVGF/6-311+G(d)), molecular orbitals (MO), and the corresponding characters of outer valence shells for ClF_2CC-(O)NCO are listed in Table 6. In accordance with the above discussion on the structure of $ClF_2CC(O)NCO$ its He(I)

dx.doi.org/10.1021/jp3096055 | J. Phys. Chem. A 2012, 116, 11586−11595

Table 3. Observed Band Positions (cm^{-1}), Relative Intensities, and Assignments for the IR Bands of the Ar-Matrix Isolated Photolysis Products of $ClF_2CC(O)NCO$ (λ = 193 nm, 20 min) and $ClF_2CC(O)N_3$ (λ > 225 nm, 10 min) at 15 K

IR (Ar matrix)				
$ClF_2CC(O)NCO$	$ClF_2CC(O)N_3$	assignment		
wavenumbers (cm^{-1})[a]	wavenumbers (cm^{-1})[a]	species	mode	calculated[b]
2281.1 (100)	2282.3 (100)	ClF_2CNCO	ν_{as}(NCO)	2359
2142.8[c]		CO	ν(CO)	
1815.4 (6)	1815.4 (3)	$ClF_2CC(O)N$	ν(CN) S/ν(CO) T	1813 S/1564 T
1463.7 (12)	1463.0 (14)	ClF_2CNCO	ν_s(NCO)	1501
1326.2 (2)	1325.5 (1)	$ClF_2CC(O)N$	ν(CO) S/ν(CC) T	1326 S/1231 T
1165.6	1166.5	$ClF_2CC(O)N$	$\nu_{as}(CF_2)$	1167 S/1143 T
1156.5 (23)	1150.5 (19)	ClF_2CNCO	$\nu_{as}(CF_2)$	1156
1138.6/1137.3 (8)	1138.6/1137.3 (6)	$ClF_2CC(O)N$	$\nu_s(CF_2)$	1150 S/1094 T
1117.2 (<1)	1116.0 (<1)	ClF_2CNCO	$\nu_s(CF_2)$	1101
1001.3 (35)	1001.7/995.7 (39)	ClF_2CNCO	$\nu_{as}(CF_2)$	965
	707.1 (1)	ClF_2CNCO	$\delta(CF_2)$	720
	667.5 (1)	ClF_2CNCO	δ(NCO)	670
588.0 (1)	595.1 (1)	ClF_2CNCO	δ(NCO)	613
	591.3 (1)	$ClF_2CC(O)N$	δ(CO)	615 T/599 S

[a]Relative intensities based on the integration of band areas are given in parentheses. [b]Calculated vibrational frequencies (cm^{-1}) at the B3LYP/6-311+(3df) level reported in ref 6 for $ClF_2CC(O)N$ are given for the singlet (S) and triplet (T) states. [c]Reference 32, 2139 cm^{-1}

Table 4. Experimental and Theoretical Structural Parameters of $ClF_2CC(O)NCO$[a]

	gauche−syn				gauche−anti			
	GED		calculations		GED		calculations	
parameter[b]	r_g	r_e, $\angle_e$	B3LYP/6-31G(d)	MP2(full)/aug-cc-pVTZ	r_g	r_e, $\angle_e$	B3LYP/6-31G(d)	MP2(full)/aug-cc-pVTZ
O1−C2	1.200(1)	1.195(1)[1]	1.203	1.199	1.197(1)	1.192(1)[1]	1.200	1.196
C2−N3	1.388(9)	1.378(9)[2]	1.396	1.385	1.384(9)	1.374(9)[2]	1.391	1.381
C2−C6	1.553(7)	1.541(7)[3]	1.546	1.529	1.561(7)	1.548(7)[3]	1.556	1.536
N3−C4	1.223(1)	1.218(1)[1]	1.227	1.222	1.221(1)	1.216(1)[1]	1.224	1.220
C4−O5	1.162(1)	1.157(1)[1]	1.165	1.161	1.164(1)	1.158(1)[1]	1.166	1.162
C6−Cl7	1.764(4)	1.756(4)[4]	1.800	1.755	1.767(4)	1.758(4)[4]	1.798	1.757
C6−F8	1.340(3)	1.331(3)[5]	1.334	1.327	1.336(3)	1.327(3)[5]	1.331	1.323
C6−F9	1.351(3)	1.343(3)[5]	1.344	1.339	1.356(3)	1.349(3)[5]	1.353	1.345
O1−C2−N3		124.8(8)[6]	126.6	127.2		121.8(8)[6]	123.9	124.2
O1−C2−C6		122.9(14)[7]	122.0	122.4		122.1(14)[7]	120.6	121.6
N3−C2−C6		112.3(16)[b]	111.4	110.5		116.1(16)[b]	115.4	114.3
C2−N3−C4		128.6(19)[8]	130.4	130.1		131.9(19)[8]	135.1	133.4
C2−C6−Cl7		109.3(8)[9]	109.4	109.1		109.5(8)[9]	109.7	109.3
C2−C6−F8		109.8(5)[10]	109.6	109.9		110.2(5)[10]	109.8	110.3
C2−C6−F9		110.0(5)[10]	110.5	110.1		109.6(5)[10]	110.3	109.7
N3−C4−O5		173.1[e]	173.0	173.1		172.5[e]	172.1	172.5
Cl7−C6−F8		110.0(3)[11]	109.3	109.9		110.2(3)[11]	109.7	110.2
Cl7−C6−F9		109.7(3)[11]	109.1	109.6		109.1(3)[11]	108.6	109.1
F8−C6−F9		108.1(15)[c]	108.9	108.2		108.1(15)[c]	108.7	108.2
O1−C2−C6−Cl7		100.6(42)[12]	102.9	108.0		127.2(91)[13]	97.0	109.1
x/%[f]		72(7)	81[d]	61[d]	28(7)	19[d]	39[d]	

[a]Distances are given in Å, valence and torsion angles are in degrees. [b]Vibrational corrections to the equilibrium structure have been calculated using B3LYP/6-31G(d) harmonic and cubic force fields. Three times standard deviations are given in parentheses. Superscript numbers 1, 2, ..., 13 represent groups, in which parameters were tied together in least-squares method by fixing differences between their values. [c]Dependent parameter. [d]Calculated from the ΔG° value on the assumption that only gauche−syn and gauche−anti conformers exist. [e]Fixed value. [f]Total structural factor Rstr = 5.4% was finally chosen for the two conformer model.

photoelectron spectrum should reflect the two weighted forms arising from the energetically most favorable gauche−syn and gauche−anti rotamers. In addition, theoretical calculations (OVGF/6-311+G(d)) for the two isomers do not predict appreciable differences in the ionization energies with respect to the experimental resolution of 30 meV (~240 cm^{-1}). For the sake of comparison calculated values of the most stable form are used in Table 6.

The vertical ionization energies observed in the photoelectron spectrum of $ClF_2CC(O)NCO$ agree with the calculated values with the OVGF method. The first band in the photoelectron spectrum is found at 11.54 eV and can be

dx.doi.org/10.1021/jp3096055 | J. Phys. Chem. A 2012, 116, 11586−11595

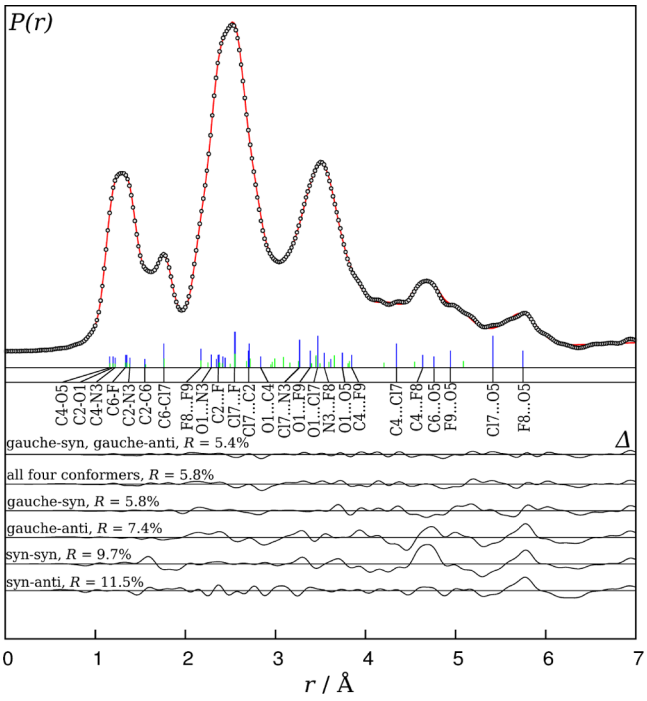

Figure 6. Experimental (open circles) and model (line) radial distribution functions. The difference curves for different models are shown below.

attributed to the ionization process from the highest occupied molecular orbital (HOMO), corresponding to the nonbonding orbital at the carbonyl oxygen atom (n_O). These ionization energies were reported to be 11.21, 12.00, and 13.20 eV for $CH_3C(O)CN$,[40] $ClF_2CC(O)CN$,[30] and $FC(O)CN$,[41] respectively, showing the intermediate inductive effect of the $ClCF_2$ group (with respect to CH_3 and F) and the influence of the electronegativity of the groups linked to C═O on the IPs (photoionization energies).

The second ionization band observed at 12.10 eV can be attributed to the π_{nb}(NCO) molecular orbital, which is in agreement with both calculations and experimental assignment. An adiabatic ionization potential value of 11.76 eV has been reported for the NCO radical using photoionization mass spectrometry.[42] For similar covalent molecules as $CH_3C(O)$-NCO this second potential was reported at 11.33 eV.[43] The third and fourth ionization bands observed at 12.50 and 12.86 eV are again in trend with $ClF_2CC(O)$-containing compounds. Thus, they are attributed to the ejection of electrons from the two nonbonding orbitals of the chlorine atom (n_{Cl}). These IPs were reported at 13.19 and 13.71 eV for the corresponding orbitals of the related molecule $ClF_2CC(O)CN$.[30] The

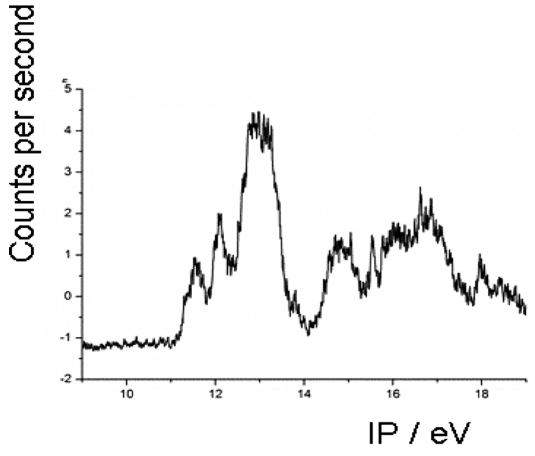

Figure 7. He(I) photoelectron spectrum (PES) of $ClF_2CC(O)NCO$.

Table 6. Experimental and Calculated Ionization Energies and MO Characters for $ClF_2CC(O)NCO$

band	exp. IP[a]	calcd. E_v[a,b]	MO	assignment
1	11.54	12.08	38	n_O
2	12.10	12.18	37	$\pi_{nb(NCO)}$
3	12.50	12.56	36	n_{Cl}
4	12.86	12.82	35	n_{Cl}
5	13.20	13.39	34	n_N
6	14.77	15.13	33	$\pi_{b(C=O)}$
7	15.53	15.87	32	n_F

[a]Energies [eV]. [b]OVGF from geometries at the B3LYP/6-311+G(d) level of approximation for the gauche−syn form.

following three ionization bands observed at 13.20, 14.77, and 15.53 eV are assigned as listed in Table 6.

Table 7. Details of the GED Experiment

parameter	short camera distance	long camera distance
nozzle-to-plate distance, mm	250.0	500.0
accelerating voltage, kV	60	60
fast electrons current, μA	0.9	1.5
electron wavelength[a], Å	0.048733	0.048597
nozzle temperature, K	293	293
residual gas pressure[b], mbar	1.6×10^{-5}	2.1×10^{-5}
exposure time, s	30	41
used s range, $Å^{-1}$	8.2 − 34.0	2.2 − 16.0
number of inflection points[c]	6	5

[a]Determined from C_6H_6 diffraction patterns measured in the same experiment. [b]During the measurement. [c]Number of inflection points on the background line.

Table 5. Selected Structural Parameters for $ClF_2CC(O)NCO$ and the Related Compounds HNCO, $H_3CC(O)NCO$, $FC(O)NCO$, and $ClC(O)NCO$

		(N)C═O	N═C(O)	C−N	C═O	<NCO	<(C/H)NC	<OCN(CO)	ref
$ClF_2CC(O)NCO$ *syn*	r_e	1.157(1)	1.218(1)	1.378(9)	1.195(1)	173.1[a]	128.6(19)	124.8(8)	this work
HNCO	r_e	1.16991(83)	1.21220(76)			173.33(20)	123.11(15)		34
$H_3CC(O)NCO$ *syn*	r_α	1.159(6)	1.199(7)	1.413(7)	1.199(6)	173.0[a]	128.2(13)	124.5(23)	35
$FC(O)NCO$ *syn*	r_a	1.154(8)	1.215(9)	1.388(4)	1.192(8)	174.6(25)	125.9(11)	128.7(6)	36
$ClC(O)NCO$ *anti*	r_a	1.139(16)	1.218(23)	1.384(6)	1.201(16)	173.4(23)	127.1(16)	124.8(15)	7

[a]Assumed parameter kept fixed during refinement.

dx.doi.org/10.1021/jp3096055 | J. Phys. Chem. A 2012, 116, 11586−11595

Photoionization Mass Spectrum. The ultraviolet photoionization mass spectrum (PIMS) of $ClF_2CC(O)NCO$ was recorded together with the photoelectron spectra and is shown in Figure 8. The PIMS confirms the identity of the sample. The spectrum of $ClF_2CC(O)NCO$ mainly shows three peaks: $C(O)NCO^+$, ClF_2C^+ ($^{35/37}Cl$ isotopomers), $F_2CC(O)N^+$, and $F_2CC(O)NCO^+$.

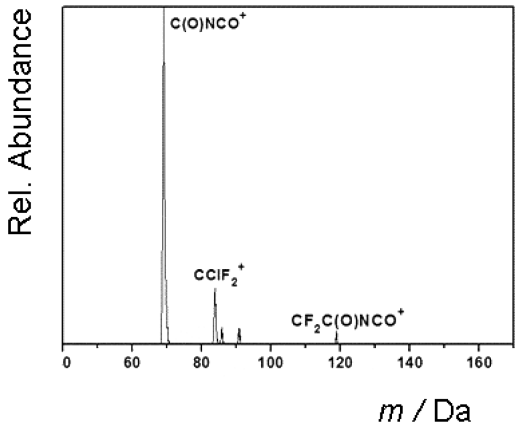

Figure 8. He(I) photoionization mass spectrum (PIMS) of $ClF_2CC(O)NCO$.

CONCLUSION

$ClF_2CC(O)NCO$ is a new nine-atomic molecule with interesting properties. This compound has been fully characterized in terms of physical, spectroscopic and structural data. It adopts gauche−syn and gauche−anti conformations in the gaseous and liquid phases both of C_1 symmetry according to vibrational spectroscopy, gas electron diffraction and quantum chemical calculations. The structural parameters are similar to those of related molecules, with some variations mainly depending on the electronic nature of the binding group R at the RC(O)NCO skeleton. The photolysis in matrix lead to both, $ClF_2CC(O)N$ and ClF_2CNCO, as photoproducts. The PE spectrum of $ClF_2CC(O)NCO$ is characterized by the first vertical ionization energy at 11.54 eV mainly corresponding to the lone-pair orbital at the carbonyl oxygen atom. Some remarkable geometrical parameters for the most stable gauche−syn conformation are the C═O double bond length of 1.195(1) Å, the N═C═O angle with a value close to 180° and the O−C−C−Cl torsion angle of 100.6(42)°.

ASSOCIATED CONTENT

Supporting Information

^{19}F and ^{13}C NMR spectra of $ClF_2CC(O)NCS$, $ClF_2CC(O)NCO$, $ClF_2CC(O)N_3$ (Figure S1 and S2); UV−vis spectra of gaseous $ClF_2CC(O)NCS$, $ClF_2CC(O)NCO$, $ClF_2CC(O)N_3$ (Figure S3), total and molecular electron scattering intensity curves (Figure S4 and S5); interatomic distances, mean square amplitudes and vibrational corrections (Tables S1 and S2); experimental Cartesian coordinates of gauche−syn and gauche−anti conformers (Tables S3 and S4). This material is available free of charge via the Internet at http://pubs.acs.org.

AUTHOR INFORMATION

Present Address

[#]Universität Salzburg, Fachbereich für Materialwissenschaften and Physik, Hellbrunnerstraße 34, 6020 Salzburg, Austria.

Notes

The authors declare no competing financial interest.

ACKNOWLEDGMENTS

The authors thank Deutsche Forschungsgemeinschaft (DFG), Alexander von Humboldt Stiftung (stipend for Y.V.V.), Deutscher Akademischer Austauschdienst (DAAD, Regional Program of Chemistry for Argentina supporting the PhD of Latin-American students in La Plata), Agencia Nacional de Promoción Científica y Técnica (ANPCYT), Consejo Nacional de Investigaciones Científicas y Técnicas (CONICET), Comisión de Investigaciones de la Provincia de Buenos Aires (CIC), Facultad de Ciencias Exactas, Universidad Nacional de La Plata (UNLP), and Universität Bielefeld for financial support. C.O.D.V. and R.M.R. acknowledge CONICET and ICCAS (Institute of Chemistry of the Chinese Academy of Sciences) for a grant to travel and stay in Beijing. C.O.D.V. thanks the Chinese Academy of Sciences for a Visiting Professorship Award for the Senior International Scientists 2011 and for the grant to travel and stay in Beijing.

REFERENCES

(1) Ulrich, H. *Chemistry and Technology of Isocyanates*, 1st ed.; John Wiley & Sons: London, 1997; p 514.
(2) Liu, Q.; De Wijn, J. R.; Van Blitterswijk, C. A. *J. Biomed. Mater. Res.* **1998**, *40*, 358−364.
(3) Alaee, M.; Livingstone, E. G.; Westwood, P. C. *J. Am. Chem. Soc.* **1993**, *115*, 2871−2876.
(4) Torrico Vallejos, S.; Erben, M. F.; Willner, H.; Boese, R.; Della Védova, C. O. *J. Org. Chem.* **2007**, *72*, 9074−9080.
(5) Zeng, X.; Beckers, H.; Willner, H. *Angew. Chem.* **2010**, *49*, 1−5.
(6) Ramos, L. A.; Zeng, X.; Ulic, S. E.; Beckers, H.; Willner, H.; Della Védova, C. O. *J. Org. Chem.* **2012**, *77*, 6456−6462.
(7) Mack, H.-G.; Oberhammer, H.; Della Védova, C. O. *J. Mol. Struct.* **1989**, *200*, 277−288.
(8) Gobbato, K. I.; Della Védova, C. O.; Mack, H.-G. *Spectrochim. Acta* **1994**, *50A*, 897−902.
(9) Curtius, T. *Ber. Dtsch. Chem. Ges.* **1850**, *23*, 3023−3033.
(10) Wang, W.; Ge, M. F.; Yao, L.; Zeng, X.; Sun, Z.; Wang, D. *Chem. Phys. Chem.* **2006**, *7* (6), 1382−1387.
(11) Gombler, W.; Willner, H. *J. Phys. E: Sci. Instrum.* **1987**, *20*, 1286−1288.
(12) Schnöckel, H. G.; Willner, H. *Infrared and Raman Spectroscopy, Methods and Applications* Plenum Press: New York, 1994; p 297.
(13) Frisch, M. J.; Trucks, G. W.; Schlegel, H. B.; Scuseria, G. E.; Robb, M. A.; Cheeseman, J. R.; Montgomery, J. A., Jr.; Vreven, T.; Kudin, K. N.; Burant, J. C.; Millam, J. M.; Iyengar, S. S.; Tomasi, J.; Barone, V.; Mennucci, B.; Cossi, M.; Scalmani, G.; Rega, N.; Petersson, G. A.; Nakatsuji, H.; Hada, M.; Ehara, M.; Toyota, K.; Fukuda, R.; Hasegawa, J.; Ishida, M.; Nakajima, T.; Honda, Y.; Kitao, O.; Nakai, H.; Klene, M.; Li, X.; Knox, J. E.; Hratchian, H. P.; Cross, J. B.; Bakken, V.; Adamo, C.; Jaramillo, J.; Gomperts, R.; Stratmann, R. E.; Yazyev, O.; Austin, A. J.; Cammi, R.; Pomelli, C.; Ochterski, J. W.; Ayala, P. Y.; Morokuma, K.; Voth, G. A.; Salvador, P.; Dannenberg, J. J.; Zakrzewski, V. G.; Dapprich, S.; Daniels, A. D.; Strain, M. C.; Farkas, O.; Malick, D. K.; Rabuck, A. D.; Raghavachari, K.; Foresman, J. B.; Ortiz, J. V.; Cui, Q.; Baboul, A. G.; Clifford, S.; Cioslowski, J.; Stefanov, B. B.; Liu, G.; Liashenko, A.; Piskorz, P.; Komaromi, I.; Martin, R. L.; Fox, D. J.; Keith, T.; Al-Laham, M. A.; Peng, C. Y.; Nanayakkara, A.; Challacombe, M.; Gill, P. M. W.; Johnson, B.; Chen, W.; Wong, M. W.; Gonzalez, C.; Pople, J. A. Gaussian 03, revision C.02; Gaussian, Inc.: Wallingford, CT, 2004.
(14) Møller, C.; Plesset, M. S. *Phys. Rev.* **1934**, *46*, 618−622.
(15) Granovsky, A. A.; *Firefly version 7.1.G*, http://classic.chem.msu.su/gran/firefly/index.html.
(16) Becke, A. D. *J. Chem. Phys.* **1993**, *98*, 5648−5652.
(17) Lee, C.; Yang, W.; Parr, R. G. *Phys. Rev. B* **1988**, *37*, 785−789.

(18) Perdew, J. P.; Burke, K.; Ernzerhof, M. *Phys. Rev. Lett.* **1996**, *77*, 3865−3868.
(19) Perdew, J. P.; Burke, K.; Ernzerhof, M. *Phys. Rev. Lett.* **1997**, *78*, 1396−1396.
(20) Ortiz, J. V. *J. Chem. Phys.* **1988**, *89*, 6348−6352.
(21) Zhao, H.; Wang, D.; Xu, G. *J. Anal. Instrum* **1992**, *4*, 23.
(22) Willet, G. D. Ph. D. Thesis; La Trobe University: Australia, 1977.
(23) Berger, R. J. F.; Hoffmann, M.; Hayes, S. A.; Mitzel, N. W. *Z. Naturforsch.* **2009**, *64b*, 1259−1268.
(24) Vishnevskiy, Y. V. *J. Mol. Struct..* **2007**, *833*, 30−41.
(25) Vishnevskiy, Y. V. *J. Mol. Struct.* **2007**, *871*, 24−32.
(26) Sipachev, V. A. *J. Mol. Struct.* **2004**, *693*, 235−240.
(27) Sipachev, V. A. *J. Mol. Struct.* **2001**, *567*−*568*, 67−72.
(28) Sipachev, V. A. *Struct. Chem.* **2000**, *11*, 167−172.
(29) Sipachev, V. A. *J. Mol. Struct.: THEOCHEM* **1985**, *121*, 143−151.
(30) Ramos, L. A.; Ulic, S. E.; Romano, R. M.; Tong, S.; Ge, M. F.; Vishnevskiy, Y. V.; Berger, R. J. F.; Mitzel, N. W.; Beckers, H.; Willner, H.; Della Védova, C. O. *Inorg. Chem.* **2011**, *50*, 9650−9659.
(31) Ramos, L. A.; Ulic, S. E.; Romano, R. M.; Tong, S.; Ge, M. F.; Beckers, H.; Willner, H.; Della Védova, C. O.; to be published.
(32) Dubost, H. *Chem. Phys.* **1976**, *12*, 139−151.
(33) Vishnevskiy, Y. V., UNEX version 1.5, http://molstruct.chemport.ru.
(34) Zinchenko, I.; Henkel, C.; Mao, R. Q. *Astron. Astrophys.* **2000**, *361* (3), 1079−1094.
(35) Mack, H.-G.; Oberhammer, H.; Della Védova, C. O. *J. Mol. Struct.* **1992**, *265*, 359−366.
(36) Mack, H.-G.; Della Védova, C. O.; Willner, H. *J. Mol. Struct.* **1993**, *291*, 197−209.
(37) Yao, L.; Ge, M. F.; Wang, W.; Zeng, X.; Sun, Z.; Wang, D. *Inorg. Chem.* **2006**, *45*, 5971−5975.
(38) Zeng, X.; Ge, M.; Sun, Z.; Wang, D. *Inorg. Chem.* **2005**, *44*, 9283−9287.
(39) Zeng, X.; Liu., F. Y.; Sun, Q.; Ge, M. F.; Zhang, J. P.; Ai, X. C.; Meng, L. P.; Zheng, S. J.; Wang, D. X. *Inorg. Chem.* **2004**, *43*, 4799−4801.
(40) Katsumata, S.; Tabayashi, K.; Sugihara, T.; Kimura, K. *J. Electron Spectros. Relat. Phen.* **2000**, *113*, 49−55.
(41) Von Niessen, W.; Fougère, S. G.; Janvier, D.; Klapstein, D. *J. Mol. Struct.* **1992**, *265*, 133−142.
(42) Ruscic, B.; Berkowitz, J. *J. Chem. Phys.* **1994**, *100*, 4498−4508.
(43) Zeng, X.; Yao, L.; Ge, M. F.; Wang, D. *J. Mol. Struct.* **2006**, *789*, 92−99.